Histol Histopathol (2022) 37: 779-789

http://www.hh.um.es

Histology and Histopathology
From Cell Biology to Tissue Engineering

ORIGINAL ARTICLE **Open Access**

MiR-19b-3p promotes tumor progression of non-small cell lung cancer via downregulating HOXA9 and predicts poor prognosis in patients

Zu-Lei Li, Dong Li and Guo-Qiang Yin

Department of Thoracic Surgery, Zibo Central Hospital, Zibo, Shandong Province, PR China

Summary. MiR-19b-3p has been reported in several types of human cancer. Nevertheless, the expression profile and biological functions of miR-19b-3p remain unclear in non-small cell lung cancer (NSCLC). The expression level of miR-19b-3p was evaluated in NSCLC tissues and cell lines using qRT-PCR. Survival analysis was performed using Kaplan-Meier curves, while the prognostic significance of miR-19b-3p was analyzed using Cox regression analysis in 80 NSCLC patients. The effects of miR-19b-3p on cell proliferation and invasion capacities were analyzed using CCK-8, crystal violet, and transwell assays. Target genes of miR-19b-3p were assessed using luciferase reporter assay, qRT-PCR, Western blot and rescue experiments. MiR-19b-3p was found to be upregulated in human NSCLC tissues and cell lines. The expression of miR-19b-3p was observed to be closely associated with TNM stage and metastasis. High expression of miR-19b-3p was found to be capable of predicting poor clinical prognosis in NSCLC patients. Whilst overexpression of miR-19b-3p was demonstrated to promote the proliferation and invasion of NSCLC cells, knockdown of miR-19b-3p showed an opposite inhibitory effect. Bioinformatics analysis and luciferase reporter assays confirmed that HOXA9 is a direct target of miR-19b-3p. Functional assays demonstrated that NSCLC cell proliferation and invasion were promoted by miR-19b-3p via negative regulation of HOXA9. Finally, overexpression of HOXA9 was shown to partially reverse the tumor promoting effect of miR-19b-3p. This study indicates that miR-19b-3p is a crucial prognostic biomarker of NSCLC, and that targeting of the miR-19b-3p/HOXA9 axis may be a promising strategy in NSCLC therapy.

Corresponding Author: Dr. Guo-Qiang Yin, M.D., Department of Thoracic Surgery, Zibo Central Hospital, No. 10 South Shanghai Road, Zibo, Shandong Province, 255000, PR China. e-mail: Guoqiangdr@163.com

DOI: 10.14670/HH-18-448

Key words: NSCLC, miR-19b-3p, HOXA9, Progression, Prognosis

Introduction

As one of the most frequently diagnosed cancers and the leading cause of death in both men and women with cancers in China, lung cancer is expected to have an increased incidence over the next decades (Mao et al., 2016). Non-small cell lung cancer (NSCLC), the most common type of lung cancer has been found to account for about ~85% of all lung carcinomas (Molina et al., 2008). Despite recent advancements in therapeutic interventions, such as surgery, chemotherapy, radiation therapy and immunotherapy, the overall 5-year survival rate of NSCLC patients remains low at only 19.7% (Donington et al., 2011; Hirsch et al., 2017; Jones and Baldwin, 2018). Recently, there has been a promising breakthrough in the treatment of lung cancer using molecular targeted therapy (Naylor et al., 2016). Hence, investigations of molecular mechanisms in NSCLC pathogenesis are important to facilitate NSCLC prevention and treatment strategies.

MicroRNAs (miRNAs) are a group of small non-coding RNAs with a length of 20-22 nucleotides that can selectively suppress gene expression through complementary binding with 3' untranslated regions (UTRs) of their target mRNAs, thus resulting in their degradation and translation suppression (Macfarlane and Murphy, 2010). Recent studies have extensively elucidated the expression of miRNAs and their biological functions in many cancers, by showing that abnormal expression of miRNAs plays numerous regulatory roles in various physiological and developmental processes, such as cell development, differentiation, apoptosis, proliferation, autophagy, and senescence (Tutar, 2014; He et al., 2017; Qadir and Faheem, 2017; Sun et al., 2018; Gupta et al., 2020). In human NSCLC, emerging evidence has shown that abnormal expression of miRNAs is associated with NSCLC initiation and progression, and that the abnormally

expressed miRNAs can be used as diagnostic or prognostic biomarkers for NSCLC patients (Zhu et al., 2017; Zhang et al., 2017).

MiR-19b-3p has been reported to play a cancer-promoting role in different cancer types, including pancreatic cancer (Song et al., 2019), renal cell carcinoma (Wang et al., 2019), intrahepatic cholangiocarcinoma (Tang et al., 2020) and colon cancer (Jiang et al., 2017). Conversely, a tumor-suppressing role of miR-19b-3p has also been reported in gastric cancer (Wei et al., 2020) and breast cancer (Jin et al., 2018). In addition, plasma miR-19b-3p has been found to be highly expressed in lung cancer patients compared to that in healthy patients (Bulgakova et al., 2018). Nevertheless, the comprehensive prognostic and biological roles of miR-19b-3p and its underlying mechanism in NSCLC remain unclear.

In this study, we found that the endogenous expression of miR-19b-3p was upregulated in NSCLC cell lines and clinical tissues, and that high expression of miR-19b-3p was associated with poor prognosis in NSCLC patients. Overexpression of miR-19b-3p was demonstrated to promote the proliferation and invasion of NSCLC cells *in vitro*, while downregulation of miR-19b-3p showed an opposite inhibitory effect. Bioinformatics analysis demonstrated that miR-19b-3p inhibited HOXA9 expression through specific 3'-UTR binding. Hence, miR-19b-3p exerts a tumor-promoting role via negative regulation of HOXA9. Taken together, our findings reveal a novel regulatory network of miR-19b-3p/HOXA9 in NSCLC, which may be used as novel prognostic and therapeutic targets.

Materials and methods

Patient samples

Tumor tissues and paired adjacent normal tissues were obtained from 80 NSCLC patients at Zibo Central Hospital (Shandong, China) between January 2011 and January 2014. NSCLC patients fulfilling the following criteria were included in this study: (1) Underwent primary surgery; (2) Without pre-surgical anti-cancer treatments like adjuvant chemotherapy or radiation treatment; (3) With all collected tumor samples being pathologically diagnosed and confirmed; and (4) With complete follow-up information including basic clinicopathological features and survival time. The follow-up of this cohort ended on July 2019. All collected samples were immediately frozen in liquid nitrogen and stored at -80°C before further analyses. A written informed consent was obtained from all patients. This study was approved by the ethics committee of Zibo Central Hospital, and was conducted in accordance with the Declaration of Helsinki.

Cell culture

Human normal lung epithelial cells (16HBE) and NSCLC cell lines (H1299, H520, and A549) were obtained from American Type Culture Collection (ATCC). Cells were cultured in RPMI-1640 culture medium (Thermo Fisher Scientific, USA) containing 10% fetal bovine serum (FBS; Gibco, Carlsbad, CA) at 37°C with 5% CO_2.

RNA extraction and reverse transcription quantitative polymerase chain reaction (RT-qPCR)

Total RNA, including miRNAs, from clinical tissue and cell line samples was extracted using TRIzol reagent (Invitrogen, Carlsbad, CA, USA). A total of 1 μg mRNA was reverse transcribed into cDNA using TaqMan microRNA Reverse Transcription kit (Applied Biosystems; Thermo Fisher Scientific, Inc., Waltham, MA, USA) in accordance with the manufacturer's protocol. RT-qPCR was conducted using SYBR-Green Kit (Takara Biotechnology Co., Ltd.) on ABI7900 LightCycler (Roche Diagnostics, Basel, Switzerland) set with the following thermal cycling conditions: 95°C for 3 min, followed by 40 cycles of 94°C for 20 sec, 55°C for 20 sec and 72°C for 30 sec. Relative expression of miR-19b-3p and HOXA9 were normalized to that of U6 and GAPDH, respectively, using the $2^{-\Delta\Delta Ct}$ method (Livak and Schmittgen, 2001). The sequences of oligonucleotides (GeneChem Co., Ltd, Shanghai, China) used for RT-qPCR reactions were as follows: 5'-AACAGAAGTTTTGCAGGTTTGCATC-3' (miR-19b-3p forward), 5'-CAGTGCAGGGTCCGAGGT-3' (miR-19b-3p reverse), 5'-CTCGCTTCGGCAGCACA-3' (U6 forward), 5'-AACGCTTCACGAATTTGCGT-3' (U6 reverse), 5'-GCTTGTGGTTCTCCTCCAGTTG-3' (HOXA9 forward), 5'-TCCCTGGTGAGGTAC ATGTTGAA-3' (HOXA9 reverse), 5'-CTGGGCTACA CTGAGCACC-3' (GAPDH forward), 5'-AAGTGGT CGTTGAGGGCAATG-3' (GAPDH reverse).

Western Blotting

A549 cells were lysed in RIPA solution (Thermo Fisher Scientific, Inc.), and the lysates were centrifuged at 10000 g for 15 minutes at 4°C according to the manufacturer's instructions. Protein concentration was determined using the Bradford reagent (Sigma). 20 μg of protein were separated on 10% SDS-PAGE, and transferred onto polyvinylidene difluoride membranes and blocked with 5 % non-fat milk for 2 h at room temperature. The blots were then immunoblotted with the indicated primary antibodies at 4°C overnight. The primary antibodies were as follows: HOXA9 (dilution, 1:1,000; cat. no. ab140631; Abcam, CA, USA) and GAPDH (dilution, 1:1,000; cat. no. 60004-1-Ig; ProteinTech Group, Inc.). Next, the membranes were incubated with corresponding horseradish peroxidase (HRP)-conjugated secondary antibody for 2 h at room temperature. Immunoreactive protein bands were visualized by chemiluminescence imaging system (Bio-Rad, USA) and subsequently quantified using Image J.

The expression levels of target proteins were normalized against GAPDH protein expression.

Cell transfection

MiR-19b-3p mimics, miR-19b-3p inhibitor and their corresponding negative controls (miR-NCs), and homeobox A9 (HOXA9)-overexpressing plasmid (pcDNA3.1-HOXA9) were designed and purchased from GeneChem Co., Ltd (Shanghai, China). NSCLC cells were seeded into six-well plates at a density of 5×10^5 cells per well and grown overnight. The cells were 60-70% confluent before being transfected using Lipofectamine 2000 (Invitrogen, Carlsbad, CA, USA) in accordance with the manufacturer's instructions. Transfected cells were further cultured for 48 h at 37°C before being used in subsequent experiments. Their sequences were as follows: miR-19b-3p mimics, 5'-AGUUUUGCAUGGAUUUGCAC-3'; negative control, 5'-UUCUCCGAACGUGUCACGUTT-3', miR-19b-3p inhibitor, 5'-UCAGUUUUGCAUGGAUUUGCACA-3'; negative control, 5' -CAGUACUUUUGUGUAG UACAA-3'.

Cell counting kit-8 (CCK-8) proliferation assays

Three replicates of transfected NSCLC cells were seeded into 96-well plates at a density of 4×10^3 cells per well, following which 10 μL of CCK-8 solution (Dojindo, Kumamoto, Japan) was added to the medium at 24, 48, 72, and 96 h before the cells were further incubated at 37°C for 2 h. Optical density (OD) values were measured at 450 nm using an automatic microplate reader (Bio-Rad Laboratories, Inc., Hercules, CA, USA).

Crystal violet assays

Three replicates of transfected NSCLC cells were seeded into six-well plates at a density of 1×10^3 cells per well, and cultured in DMEM with 10% FBS. The cell culture medium was changed every three days for two weeks. Cells were subsequently stained with crystal violet for 15 min at room temperature. Ten minutes later, the fixed cells were washed with phosphate-buffered saline (PBS) and photographed. Optical density (OD) values were measured at 570 nm using an automatic microplate reader (Bio-Rad Laboratories, Inc., Hercules, CA, USA).

Tranwell assays

The invasion ability of transfected NSCLC cells was examined by transwell assays using polyethylene terephthalate membranes (24-well inserts; 8.0 μm; Corning Inc.). A total of 1×10^5 cells in DMEM without serum were seeded in the upper chamber and the lower chamber was filled with 500 μL DMEM supplemented with 20% FBS. Membranes were precoated with 50 μl Matrigel (BD Biosciences) at 37°C for 4 h. Cells were cultured at 5% CO_2 and 37°C for 48 hours. Cells that have migrated or invaded the bottom of the membrane were fixed with 4% paraformaldehyde for 10 min and then stained with 1% crystal violet for 5 min at room temperature. Cells were counted in 5 randomly selected fields under a light microscope (Leica Microsystems GmbH, Wetzlar, Germany) at ×400 magnification.

Luciferase reporter assays

Amplified 3'-UTR of HOXA9 was subcloned into pmirGLO luciferase vector (GeneChem, Shanghai, China) to generate wild type HOXA9 3'-UTR plasmid construct (HOXA9-WT). Site-directed mutation of miR-19b-3p binding sites in HOXA9 3'-UTR (HOXA9-MUT) was conducted on GeneTailor™ Site-Directed Mutagenesis System (Invitrogen, Carlsbad, CA, USA). A549 cell lines were co-transfected with the constructed plasmids and miRNAs (miR-19b-3p mimic or mi-NC) with Lipofectamine® 2000 (Invitrogen; Thermo Fisher Scientific, Inc.). Transfected cells were incubated for 48 h before being lysed. Reporter activities were determined on a dual-luciferase reporter assay system (Promega, Madison, WI, USA).

Statistical analyses

All data are expressed as mean ± standard deviation. Statistical evaluations were performed using SPSS 20.0 (IBM SPSS Inc., Chicago, IL, USA). Differences between two groups were analyzed using Student's t-test. Categorical data were compared using chi-square test. Comparisons of multiple groups were analyzed using the ANOVA followed by Dunnett's test. Overall survival (OS) and recurrence-free survival (RFS) of patients with NSCLC were evaluated using Kaplan-Meier curves. Prognostic factors were assessed using Cox regression proportional hazards analysis. Correlation analysis was performed using Pearson method. Differences were considered to be significant when $P<0.05$.

Results

MiR-19b-3p is upregulated in NSCLC and is associated with poor prognosis in patients with NSCLC

To primarily explore whether miR-19b-3p is associated with NSCLC progression, the expression levels of miR-19b-3p in 80 pairs of NSCLC tissues and paired adjacent normal tissues were evaluated using RT-qPCR. Our results showed that miR-19b-3p expression was upregulated in primary NSCLC tissues compared to that in normal tissues ($P<0.01$, Fig. 1A). Next, the expression levels of miR-19b-3p were assessed in several NSCLC cell lines (A549, H520 and H1299) and human normal lung epithelial cells (16HBE). As shown in Fig. 1B, miR-19b-3p expression was significantly higher in NSCLC cell lines than that in 16HBE (all

$P<0.001$).

The potential association between miR-19b-3p expression and clinicopathological characteristics of NSCLC was analyzed. With the median value of miR-19b-3p expression in tumor tissues as the cut-off value, we divided the 80 NSCLC patients into two groups: low miR-19b-3p expression group (below the median, 40 patients) and high miR-19b-3p expression group (above the median, 40 patients). As shown in Table 1, miR-19b-3p expression levels had an association with clinicopathological data, including tumor size ($P=0.014$), TNM stage ($P<0.001$) and lymph node metastasis ($P=0.007$). Subsequently, the role of miR-19b-3p in the prognosis of NSCLC patients was also analyzed using Kaplan-Meier curves. Our results showed that NSCLC patients with high miR-19b-3p expression were associated with poor OS (Fig. 1C; $P=0.024$) and RFS (Fig. 1D; $P=0.04$) compared with patients with low miR-19b-3p expression. Consistently, univariate analysis showed that miR-19b-3p expression was associated with OS (Table 2, $P=0.004$) and RFS (Table 3, $P=0.006$). Using parameters that were significant in univariate analyses as covariates, miR-19b-3p expression level was found to be significantly associated with OS (HR=2.263, $P=0.019$, Table 2) and RFS (HR=2.654, $P=0.035$, Table 3). Taken together, our data indicated that miR-19b-3p is an independent prognostic factor in NSCLC patients.

MiR-19b-3p induces the proliferation and invasion of NSCLC cells

Next, we further investigated the biological functions of miR-19b-3p in NSCLC tumor progression. Firstly, we overexpressed or knocked-down the expression of miR-19b-3p in A549 cells transfected with miR-19b-3p mimics or inhibitors. The transfection efficacy in A549 cells was confirmed by qRT-PCR analysis ($P<0.001$, Fig. 2A), following which cell

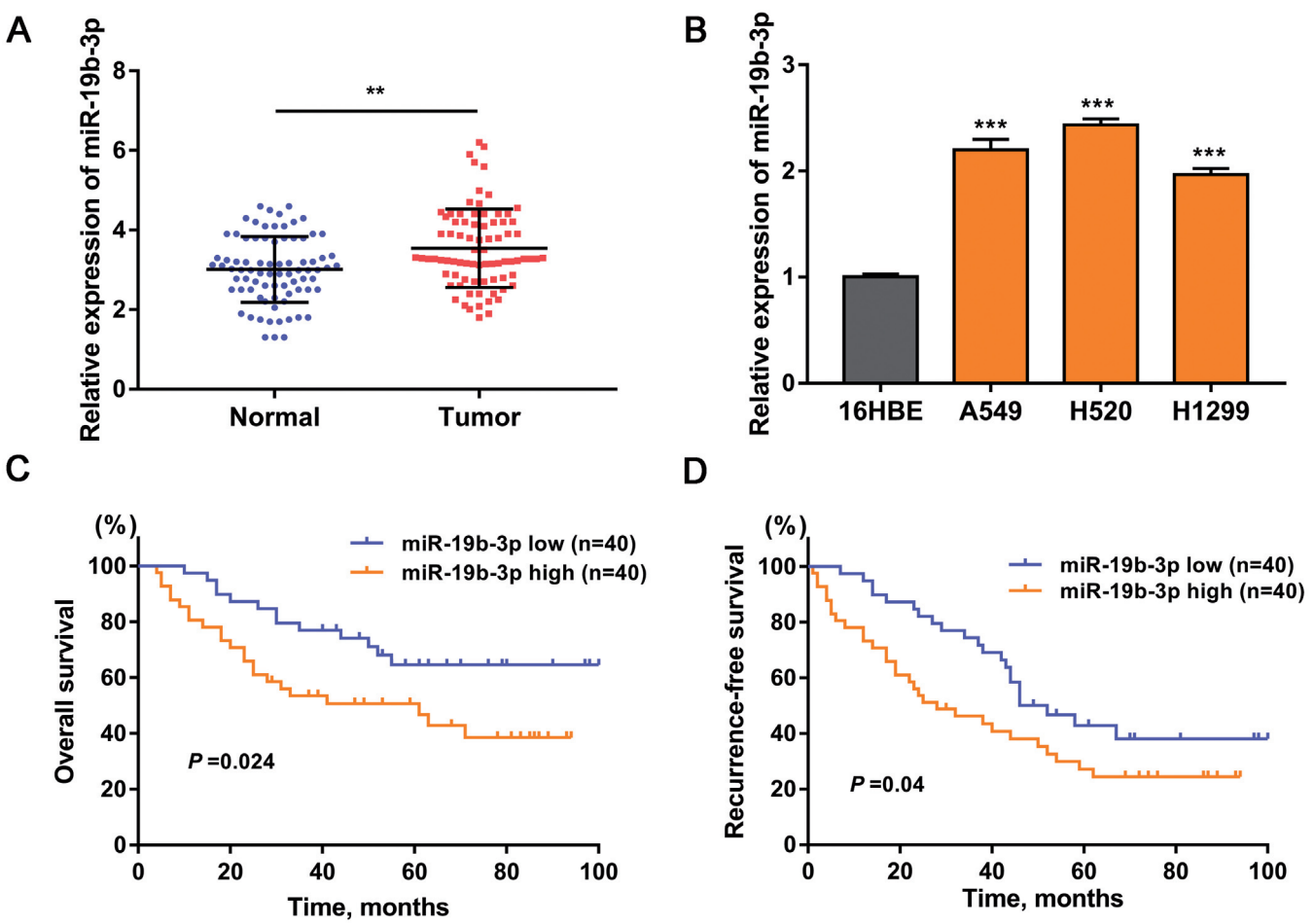

Fig. 1. Increased miR-19b-3p expression levels in NSCLC are associated with clinical prognosis. **A.** RT-qPCR analysis of miR-19b-3p expression in 80 pairs of NSCLC tissues and adjacent normal tissues. **B.** RT-qPCR analysis of miR-19b-3p expression in three NSCLC cell lines (A549, H520, and H1299) and human normal lung epithelial cells (16HBE). **C, D.** Kaplan-Meier analysis of overall survival **(C)** and recurrence-free survival **(D)** curves of NSCLC patients stratified by miR-19b-3p expression. $^{**}P<0.01$, $^{***}P<0.001$. NSCLC, non-small cell lung cancer; RT-qPCR, reverse transcription quantitative polymerase chain reaction.

proliferation capacity was evaluated by CCK-8 and crystal violet assays. As shown in Fig. 2B,C, whilst miR-19b-3p mimics significantly promoted cell proliferation, miR-19b-3p inhibitor showed an inhibitory effect on cell proliferation compared to that in respective controls. Next, the invasive capacity of A549 cells was analyzed by transwell assays. As shown in Fig. 2D, miR-19b-3p mimics notably promoted cell invasion, whereas miR-19b-3p inhibitor suppressed cell proliferation compared to that in respective controls. Taken together, miR-19b-3p increases the proliferation and invasion capabilities of NSCLC cells *in vitro*.

HOXA9 is a direct target of miR-19b-3p

Candidate target genes of miR-19b-3p were analyzed using miRNA target prediction software packages on miRNA.org (www.microrna.org/microrna/home.do) and starBase v2.0 (http://starbase.sysu.edu.cn/index.php). Our bioinformatics prediction indicated that HOXA9 is a potential target gene of miR-19b-3p. The predicted binding sequence of miR-19b-3p and HOXA9 3' UTR are shown in Fig. 3A. Next, we examined the luciferase activity of wild-type HOXA9 (HOXA9-WT) or mutant-type HOXA9 (HOXA9-MUT) in cells transfected with miR-19b-3p mimics. As shown in Fig. 3B, our results showed that the luciferase activity of HOXA9-WT but not HOXA9-MUT was decreased by miR-19b-3p mimics. To further determine whether miR-19b-3p regulates the translation of HOXA9, we transfected A549 cells with miR-19b-3p mimic and NC mimic, and with miR-19b-3p inhibitor and NC inhibitor. As shown in Fig. 3C, whilst the mRNA expression levels of HOXA9 were significantly decreased in A549 cells transfected with miR-19b-3p mimics, those in A549 cells transfected with miR-19b-3p inhibitors were conversely increased. Similarly, the protein levels of HOXA9 were observed to be decreased in A549 cells transfected with miR-19b-3p mimics, while those in A549 cells transfected with miR-19b-3p inhibitors were found to be increased (Fig. 3D). Moreover, correlation analysis demonstrated that HOXA9 mRNA expression was negatively correlated with miR-19b-3p mRNA expression in the 80 tumor samples of NSCLC patients (p<0.001, Fig. 3E). Similarly, the association between HOXA9 mRNA expression and clinicopathological characteristics of NSCLC was explored. Our results showed that HOXA9 mRNA expression was significantly downregulated in primary NSCLC tissues compared to that in normal tissues (P<0.01, Fig. 3F). Then, the 80 NSCLC patients were separated into two groups based on the median value of HOXA9 expression

Table 1. Comparison of clinicopathological features between NSCLC tumors with high miR-19b-3p expression (N=40) and tumors with low miR-19b-3p expression (N=40).

Parameters	Patients (n=80)	miR-19b-3p, N (%) High expression (n=40)	Low expression (n=40)	*P*-value
Age, years				0.502
<55	39 (48.8)	18 (45.0)	21 (52.5)	
≥55	41 (51.2)	22 (55.0)	19 (47.5)	
Gender				0.648
Male	48 (60.0)	25 (62.5)	23 (57.5)	
Female	32 (40.0)	15 (37.5)	17 (42.5)	
Smoking status				0.284
Non-smoker	18 (22.5)	7 (17.5)	11 (27.5)	
Smokers	62 (77.5)	33 (82.5)	29 (72.5)	
Tumor size (cm)				0.014*
<3	39 (48.8)	14 (35.0)	25 (62.5)	
≥3	41 (51.2)	26 (65.0)	15 (37.5)	
TNM stage				<0.001*
Early stage: I-II	38 (47.5)	11 (27.5)	27 (67.5)	
Advanced stage: III	42 (52.5)	29 (72.5)	13 (32.5)	
Pathology				0.485
Adenocarcinoma	29 (36.3)	16 (40.0)	13 (32.5)	
Squamous cell carcinoma	51 (63.7)	24 (60.0)	27 (67.5)	
Lymph node metastasis				0.007*
Yes	38 (47.5)	25 (62.5)	13 (32.5)	
No	42 (52.5)	15 (37.5)	27 (67.5)	

NSCLC, non-small cell lung cancer; TNM, tumor (T), the extent of spread to the lymph nodes (N), and the presence of metastasis (M). *P<0.05.

Table 2. Univariate and multivariate cox proportional analyses of prognostic factors associated with overall survival in NSCLC patients.

Variables	Univariate		Multivariate	
	HR (95% CI)	*P*-value	HR (95% CI)	*P*-value
Age, ≥55 vs. <55	1.141 (0.651-1.851)	0.331		
Gender, male vs. female	0.901 (0.692-1.669)	0.562		
Smoking status, smokers vs. non-smoker	1.856 (0.854-2.657)	0.365		
Tumor size, ≥3 vs. <3	1.951 (0.854-2.865)	0.132		
TNM stage, advanced vs. early	3.215 (1.651-4.985)	0.001*	2.985 (1.524-4.584)	0.013*
Pathology, adenocarcinoma vs. squamous cell carcinoma	1.217 (0.870-1.653)	0.347		
Lymph node metastasis, yes vs. no	3.564 (2.785-4.865)	0.013*	2.121 (1.354-3.451)	0.031*
MiR-19b-3p expression, high vs. low	3.553 (2.223-4.831)	0.004*	2.263 (1.336-3.687)	0.019*

NSCLC, non-small cell lung cancer; TNM, tumor (T), the extent of spread to the lymph nodes (N), and the presence of metastasis (M); HR, hazard ratio; CI, confidence interval. *P<0.05.

in tumor tissues. As shown in Table 4, HOXA9 expression levels had an association with clinicopathological data, including tumor size (P=0.001) and TNM stage (P=0.007). The Kaplan-Meier curves showed that NSCLC patients with high HOXA9 expression were associated with better OS (Fig. 3G; P=0.013) and RFS (Fig. 3H; P=0.049) compared with patients with low HOXA9 expression.

HOXA9 reverses the miR-19b-3p-induced effects in NSCLC cells

To further determine whether miR-19b-3p exerts its biological roles through HOXA9, rescue assays were conducted in A549 cells. HOXA9 was overexpressed using pcDNA3.1-HOXA9 in A549 cells transfected with miR-19b-3p. The transfection efficacy was confirmed

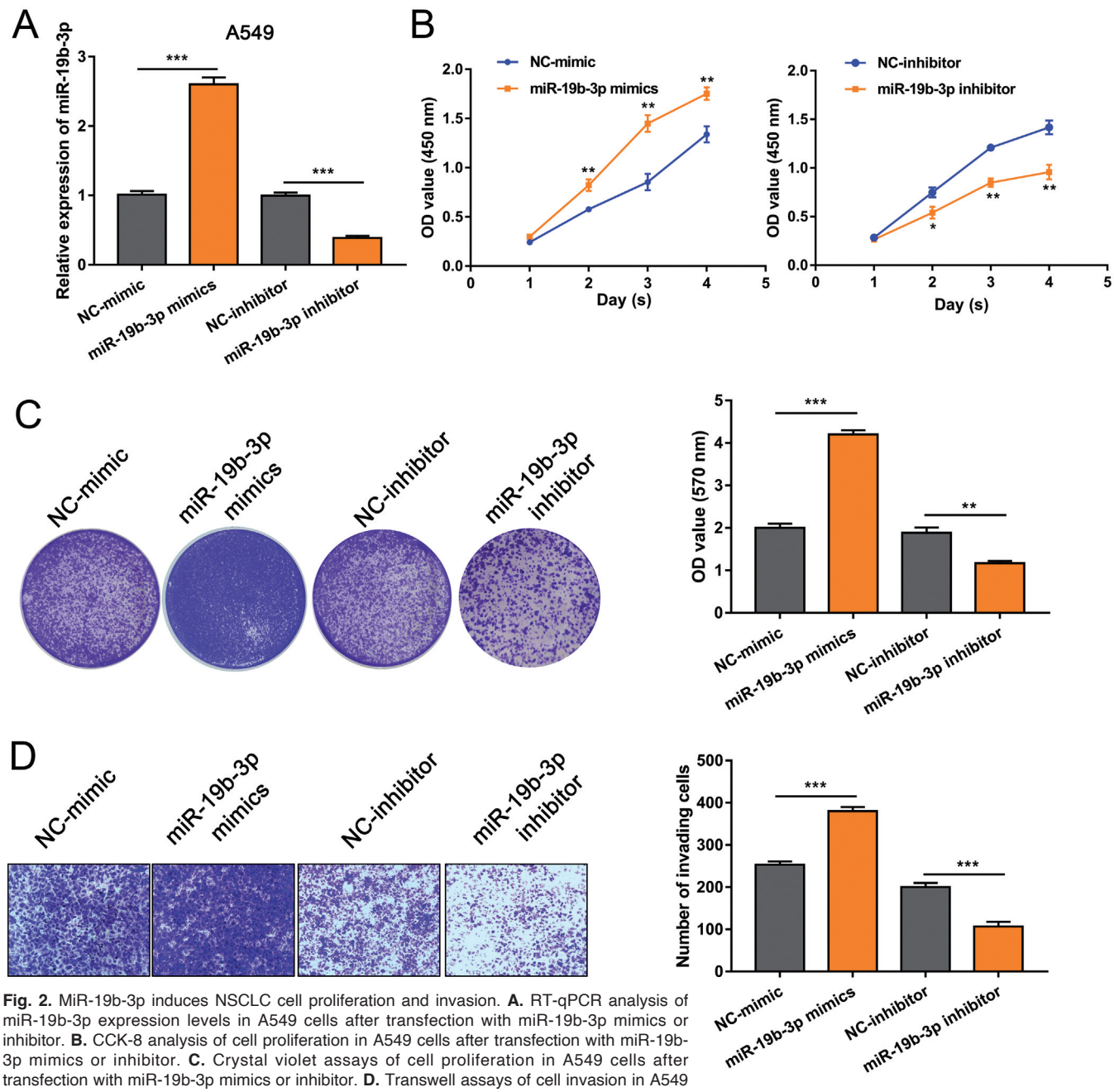

Fig. 2. MiR-19b-3p induces NSCLC cell proliferation and invasion. **A.** RT-qPCR analysis of miR-19b-3p expression levels in A549 cells after transfection with miR-19b-3p mimics or inhibitor. **B.** CCK-8 analysis of cell proliferation in A549 cells after transfection with miR-19b-3p mimics or inhibitor. **C.** Crystal violet assays of cell proliferation in A549 cells after transfection with miR-19b-3p mimics or inhibitor. **D.** Transwell assays of cell invasion in A549 cells after transfection with miR-19b-3p mimics or inhibitor. *P<0.05, **P<0.01, ***P<0.001. NSCLC, non-small cell lung cancer. x 100.

Table 3. Univariate and multivariate cox proportional analyses of prognostic factors associated with recurrence-free survival in NSCLC patients.

Variables	Univariate		Multivariate	
	HR (95% CI)	*P*-value	HR (95% CI)	*P*-value
Age, ≥55 vs. <55	1.041 (0.598-1.795)	0.221		
Gender, male vs. female	1.065 (0.715-1.769)	0.235		
Smoking status, smokers vs. non-smoker	1.775 (0.987-2.251)	0.165		
Tumor size, ≥3 vs. <3	1.864 (0.754-2.745)	0.115		
TNM stage, advanced vs. early	3.335 (1.791-4.655)	<0.001*	2.585 (1.365-4.331)	0.001*
Pathology, adenocarcinoma vs. squamous cell carcinoma	1.012 (0.704-1.771)	0.546		
Lymph node metastasis, yes vs. no	3.121 (2.545-4.687)	0.001*	2.654 (1.654-3.658)	0.018*
MiR-19b-3p expression, high vs. low	3.219 (2.102-4.654)	0.006*	2.654 (1.854-3.591)	0.035*

NSCLC, non-small cell lung cancer; TNM, tumor (T), the extent of spread to the lymph nodes (N), and the presence of metastasis (M); HR, hazard ratio; CI, confidence interval. *P<0.05.

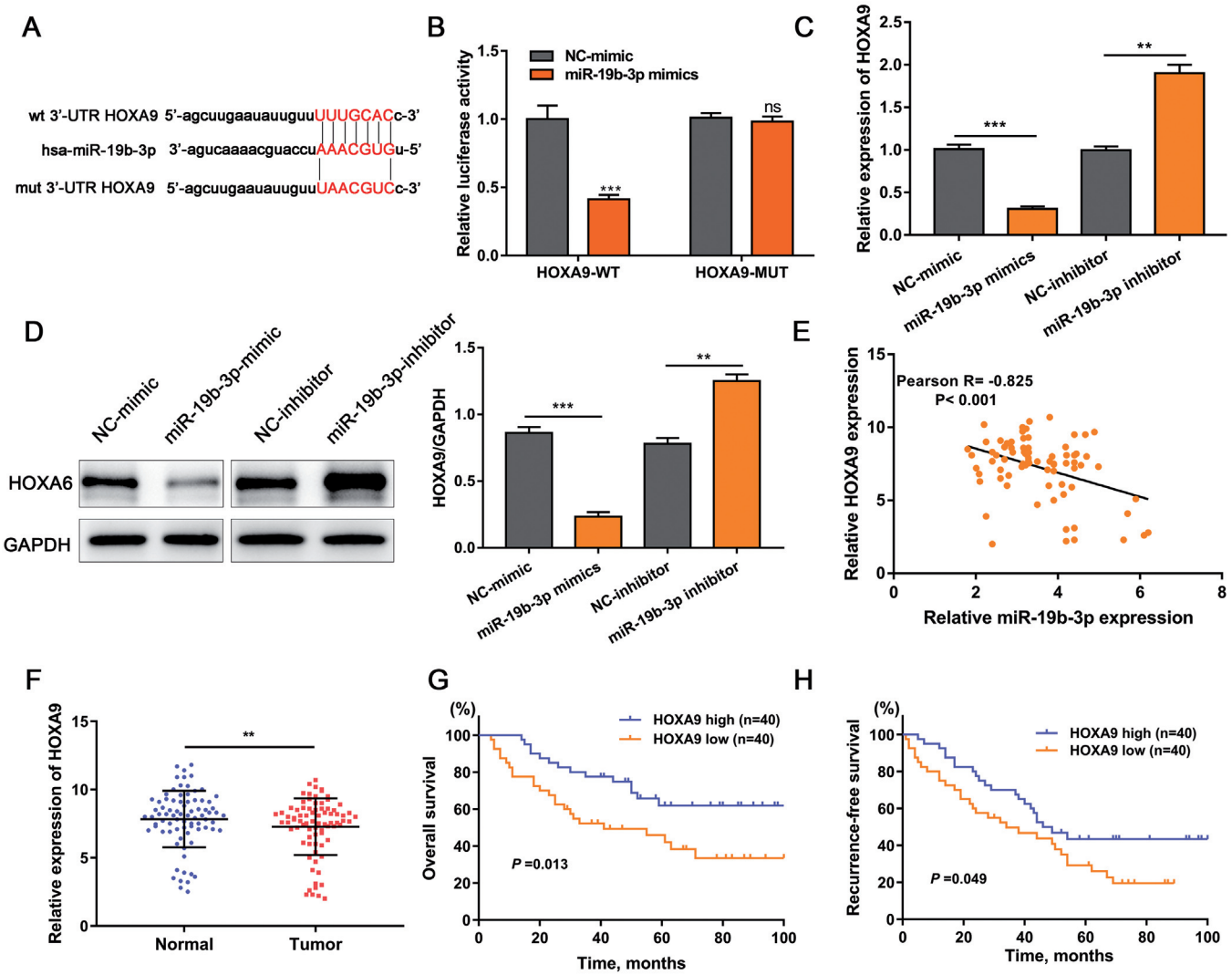

Fig. 3. HOXA9 is a direct target of miR-19b-3p. **A.** Potential associating sites of HOXA9 in the 3′-UTR region with miR-19b-3p. **B.** Luciferase reporter assays in A549 cells after transfection of miR-19b-3p mimics. **C.** RT-qPCR analysis of HOXA9 expression levels in A549 cells after transfection with miR-19b-3p mimics or inhibitor. **D.** Western bolt analysis of HOXA9 expression levels in A549 cells after transfection with miR-19b-3p mimics or inhibitor. **E.** Pearson correlation analysis between miR-19b-3p and HOXA9 expression levels in clinical samples of NSCLC patients. **F.** RT-qPCR analysis of HOXA9 expression in 80 pairs of NSCLC tissues and adjacent normal tissues. **G, H.** Kaplan-Meier analysis of overall survival **(G)** and recurrence-free survival **(H)** curves of NSCLC patients stratified by HOXA9 expression. **P<0.01, ***P<0.001, ns, not significant. RT-qPCR, reverse transcription quantitative polymerase chain reaction; NSCLC, non-small cell lung cancer.

using western blot (Fig. 4A). CCK8 and crystal violet assays showed that overexpression of HOXA9 reversed the miR-19b-3p mimics-induced effect of cell proliferation (Fig. 4B,C). Meanwhile, transwell assays demonstrated that HOXA9 overexpression reversed the invasion potential of miR-19b-3p-overexpressing A549 cells (Fig. 4D). Taken together, our data demonstrated that miR-19b-3p is a modulator of HOXA9 in NSCLC.

Discussion

An increasing number of miRNAs with critical biological functions in the progression of NSCLC that can be used as diagnostic or prognostic biomarkers have recently been identified. For instance, Zhu and colleagues have developed a serum kit containing 4 miRNAs (miR-23b, miR-221, miR-148b and miR-423-3p) that can effectively distinguish lung cancer patients from healthy individuals (Gupta et al., 2020). In addition, a series of miRNAs, such as miR-148a (Chen et al., 2017), miR-218 (Yang et al., 2017), miR-21 (Yuan et al., 2018) have been identified to be capable of predicting favorable or poor prognosis in NSCLC patients.

A number of previous studies have demonstrated the expression profiles of miR-19b-3p in multiple human cancers. Tang and colleagues have shown that, in intrahepatic cholangiocarcinoma (ICC), miR-19b-3p facilitates cell proliferation and epithelial-mesenchymal transition, but inhibits cell apoptosis and therefore can be used as a crucial biomarker for ICC diagnosis (Tang et al., 2020). Meanwhile, Jiang and colleagues have demonstrated that miR-19b-3p plays a tumor promoting role in colon cancer via bioinformatics and experimental analyses (Jiang et al., 2017). Zhao and colleagues found that miR-19b promotes breast cancer metastasis through targeting myosin regulatory light chain interacting protein (MYLIP) (Zhao et al., 2017). Conversely, Jin and colleagues have reported that miR-19b-3p inhibits the proliferation of breast cancer and plays a tumor suppressor role (Jin et al., 2018). In this study, we documented that miR-19b-3p was upregulated in human NSCLC tissues and cell lines. Moreover, we demonstrated that the expression of miR-19b-3p was closely associated with TNM stage and metastasis. Notably, high expression of miR-19b-3p was found to be capable of predicting poor clinical prognosis in NSCLC patients. These findings demonstrated the prognostic value of miR-19b-3p in NSCLC patients. Subsequently, we overexpressed/knocked-down the expression of miR-19b-3p in NSCLC cell lines using miR-19b-3p mimics/inhibitors, respectively. Then, the effects of miR-19b-3p on cell proliferation and invasion were investigated. Our results demonstrated that overexpression of miR-19b-3p promoted the proliferation and invasion of NSCLC cells, whereas knockdown of miR-19b-3p showed an opposite inhibitory effect.

Homeobox A9 (HOXA9), as one member of the HOX gene family, is primarily identified in the regulation of embryonic development and in the maintenance of hematopoietic stem cells, with a role either as an oncogene or as a tumor suppressor in various tumors (Faber et al., 2009; Gilbert et al., 2010; Smith et al., 2011). For instance, Ko et al. indicated that HOXA9 contributes to poor outcomes in cervical cancer in part by promoting intraperitoneal dissemination via its induction of P-cadherin (Ko and Naora, 2014). Bhatlekar et al. reported that HOXA9 is up-regulated in colon cancer tissues and promotes self-renewal of colon cancer stem cells (Bhatlekar et al., 2018). Hwang et al. demonstrated that HOXA9 inhibits migration of lung cancer cells and its hypermethylation is an independent prognostic factor for recurrence-free survival in non-smokers with NSCLC (Hwang et al., 2015). Han and colleagues have reported that, in cutaneous squamous cell carcinoma, HOXA9 is significantly downregulated and is identified as a tumor suppressor (Han et al., 2019). Studies have shown that HOXA9 is regulated by miRNAs in different tumors (Xu et al., 2019; Xia et al., 2019). Xu and colleagues have reported that miRNA-186-5p may inhibit cell proliferation and metastasis of esophageal cancer through the regulation of HOXA9 (Xu et al., 2019). Additionally, miR-652 has been reported to promote cell proliferation and migration via HOXA9 in uveal melanoma (Xia et al., 2019). Here, through bioinformatics analyses, we

Table 4. Comparison of clinicopathological features between NSCLC tumors with high HOXA9 mRNA expression (N=40) and tumors with low HOXA9 mRNA expression (N=40).

Parameters	Patients (n=80)	HOXA9, N (%) Low expression (n=40)	HOXA9, N (%) High expression (n=40)	*P*-value
Age, years				0.117
<55	39 (48.8)	16 (40.0)	23 (57.5)	
≥55	41 (51.2)	24 (60.0)	17 (42.5)	
Gender				0.068
Male	48 (60.0)	28 (70.0)	20 (50.0)	
Female	32 (40.0)	12 (30.0)	20 (50.0)	
Smoking status				1.000
Non-smoker	18 (22.5)	9 (22.5)	9 (22.5)	
Smokers	62 (77.5)	31 (77.5)	31 (77.5)	
Tumor size (cm)				0.001*
<3	39 (48.8)	12 (30.0)	27 (67.5)	
≥3	41 (51.2)	28 (70.0)	13 (32.5)	
TNM stage				0.007*
Early stage: I-II	38 (47.5)	13 (32.5)	25 (62.5)	
Advanced stage: III	42 (52.5)	27 (67.5)	15 (37.5)	
Pathology				0.485
Adenocarcinoma	29 (36.3)	13 (32.5)	16 (40.0)	
Squamous cell carcinoma	51 (63.7)	27 (67.5)	24 (60.0)	
Lymph node metastasis				0.654
Yes	38 (47.5)	20 (50.0)	18 (45.0)	
No	42 (52.5)	20 (50.0)	22 (55.0)	

NSCLC, non-small cell lung cancer; TNM, tumor (T), the extent of spread to the lymph nodes (N), and the presence of metastasis (M). *$P<0.05$.

predicted that miR-19b-3p may negatively regulate HOXA9 expression via direct binding to its 3'-UTR. The interaction between miR-19b-3p and HOXA9 was experimentally confirmed by luciferase reporter assays. Furthermore, HOXA9 expression was found to be negatively associated with miR-19b-3p expression in NSCLC tissues. To our knowledge, this is the first report that demonstrates the negative regulation of HOXA9 expression by miR-19b-3p in NSCLC. Finally, our rescue experiments validated that HOXA9 overexpression can partially abrogate the tumor promoting effects of miR-19b-3p.

In conclusion, this study demonstrates that miR-19b-3p is upregulated in NSCLC and is associated with poor prognosis. Exogenous miR-19b-3p expression promotes the malignancy of NSCLC *in vitro* through the negative regulation of HOXA9 expression. Thus, our results suggest a novel potential prognostic and therapeutic

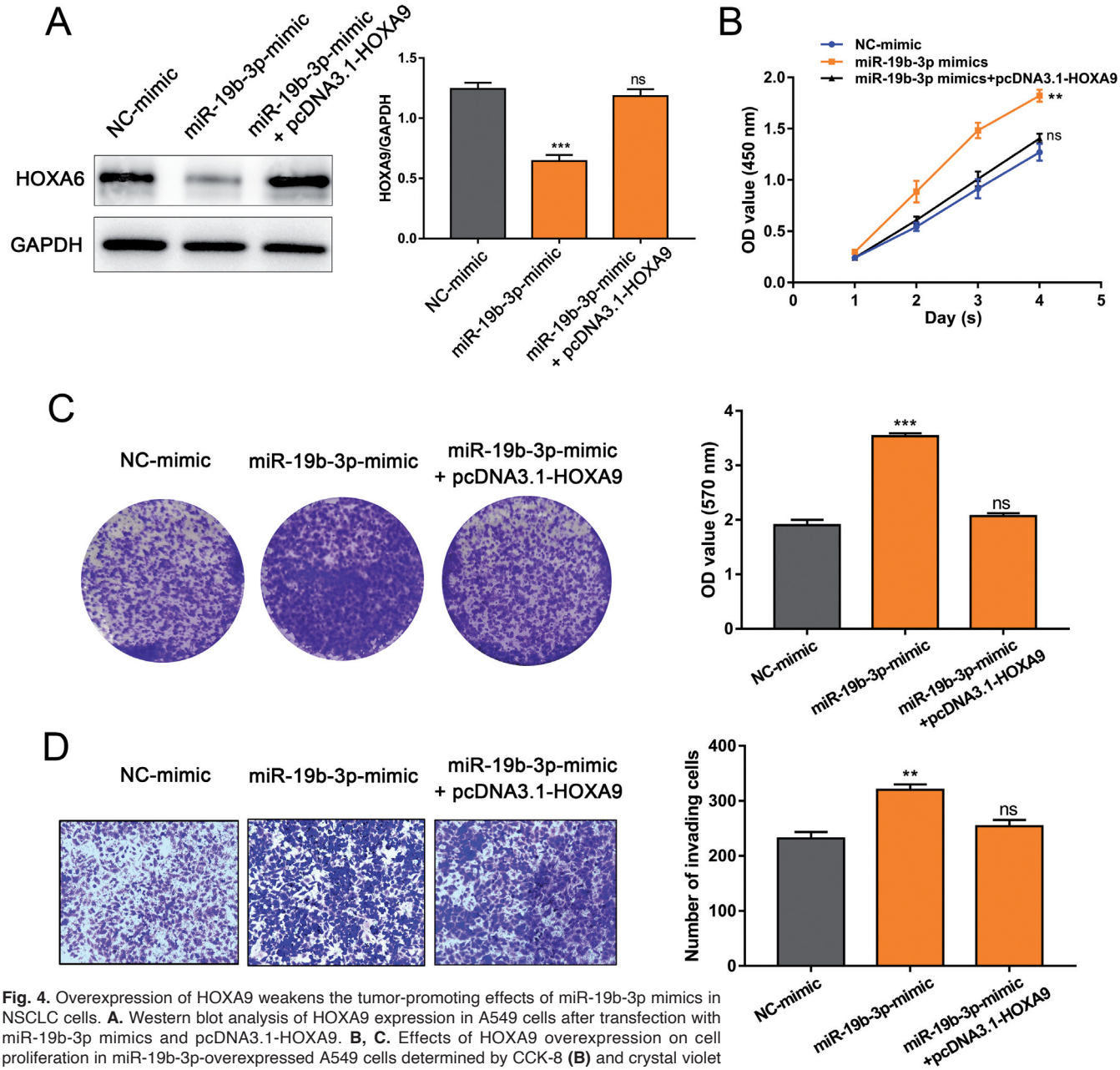

Fig. 4. Overexpression of HOXA9 weakens the tumor-promoting effects of miR-19b-3p mimics in NSCLC cells. **A.** Western blot analysis of HOXA9 expression in A549 cells after transfection with miR-19b-3p mimics and pcDNA3.1-HOXA9. **B, C.** Effects of HOXA9 overexpression on cell proliferation in miR-19b-3p-overexpressed A549 cells determined by CCK-8 **(B)** and crystal violet **(C)** assays. **D.** Effects of HOXA9 overexpression on cell invasion in miR-19b-3p-overexpressed A549 cells determined by transwell assays. ***P*<0.01, ****P*<0.001, ns, not significant. NSCLC, non-small cell lung cancer. x 100.

value of miR-19b-3p/HOXA9 in NSCLC.

Acknowledgements. Not applicable.

Funding. Not applicable.

Conflict of interest statement. No conflict of interests was declared in this study.

Data availability statement. All data generated in this study will be made available on reasonable request.

Author's contributions. Zu-Lei Li, Dong Li, and Guo-Qiang Yin conducted the experiments, Guo-Qiang Yin designed the research, Zu-Lei Li analyzed the data, and the manuscript was drafted by Zu-Lei Li, Dong Li, and Guo-Qiang Yin.

References

Bhatlekar S., Viswanathan V., Fields J.Z. and Boman B.M. (2018). Overexpression of HOXA4 and HOXA9 genes promotes self-renewal and contributes to colon cancer stem cell overpopulation. J. Cell Physiol. 233, 727-735.

Bulgakova O., Zhabayeva D., Kussainova A., Pulliero A., Izzotti A. and Bersimbaev R. (2018). miR-19 in blood plasma reflects lung cancer occurrence but is not specifically associated with radon exposure. Oncol. Lett. 15, 8816-8824.

Chen Y., Min L., Ren C., Xu X., Yang J., Sun X., Wang T., Wang F., Sun C. and Zhang X. (2017). miRNA-148a serves as a prognostic factor and suppresses migration and invasion through Wnt1 in non-small cell lung cancer. PLoS One 12, e0171751.

Donington J.S., Koo C.W. and Ballas M.S. (2011). Novel therapies for non-small cell lung cancer. J. Thorac. Imaging. 26, 175-185.

Faber J., Krivtsov A.V., Stubbs M.C., Wright R., Davis T.N., van den Heuvel-Eibrink M., Zwaan C.M., Kung A.L. and Armstrong S.A. (2009). HOXA9 is required for survival in human MLL-rearranged acute leukemias. Blood 113, 2375-2385.

Gilbert P.M., Mouw J.K., Unger M.A., Lakins J.N., Gbegnon M.K., Clemmer V.B., Benezra M., Licht J.D., Boudreau N.J., Tsai K.K., Welm A.L., Feldman M.D., Weber B.L. and Weaver V.M. (2010). HOXA9 regulates BRCA1 expression to modulate human breast tumor phenotype. J. Clin. Invest. 120, 1535-1550.

Gupta S., Silveira D.A. and Mombach J.C.M. (2020). Towards DNA-damage induced autophagy: A Boolean model of p53-induced cell fate mechanisms. DNA Repair (Amst). 96, 102971.

Han S., Li X., Liang X. and Zhou L. (2019). HOXA9 transcriptionally promotes apoptosis and represses autophagy by targeting NF-κB in cutaneous squamous cell carcinoma. Cells 8, 1360.

He X., Yang A., McDonald D.G., Riemer E.C., Vanek K.N., Schulte B.A. and Wang G.Y. (2017). MiR-34a modulates ionizing radiation-induced senescence in lung cancer cells. Oncotarget 8, 69797-69807.

Hirsch F.R., Scagliotti G.V., Mulshine J.L., Kwon R., Curran W.J. Jr, Wu Y.L. and Paz-Ares L. (2017). Lung cancer: current therapies and new targeted treatments. Lancet 389, 299-311.

Hwang J.A., Lee B.B., Kim Y., Hong S.H., Kim Y.H., Han J., Shim Y.M., Yoon C.Y., Lee Y.S. and Kim D.H. (2015). HOXA9 inhibits migration of lung cancer cells and its hypermethylation is associated with recurrence in non-small cell lung cancer. Mol. Carcinog. 54 (Suppl. 1), E72-80.

Jiang T., Ye L., Han Z., Liu Y., Yang Y., Peng Z. and Fan J. (2017). miR-19b-3p promotes colon cancer proliferation and oxaliplatin-based chemoresistance by targeting SMAD4: validation by bioinformatics and experimental analyses. J. Exp. Clin. Cancer Res. 36, 131.

Jin J., Sun Z., Yang F., Tang L., Chen W. and Guan X. (2018). miR-19b-3p inhibits breast cancer cell proliferation and reverses saracatinib-resistance by regulating PI3K/Akt pathway. Arch. Biochem. Biophys. 645, 54-60.

Jones G.S. and Baldwin D.R. (2018). Recent advances in the management of lung cancer. Clin. Med. (Lond). 18 (Suppl 2), s41-s46.

Ko S.Y. and Naora H. (2014). HOXA9 promotes homotypic and heterotypic cell interactions that facilitate ovarian cancer dissemination via its induction of P-cadherin. Mol. Cancer 13, 170.

Livak K.J. and Schmittgen T.D. (2001). Analysis of relative gene expression data using real-time quantitative PCR and the 2(-Delta Delta C(T)) method. Methods 25, 402-408.

Macfarlane L.A. and Murphy P.R. (2010). MicroRNA: Biogenesis, function and role in cancer. Curr. Genomics 11, 537-561.

Mao Y., Yang D., He J. and Krasna M.J. (2016). Epidemiology of lung cancer. Surg. Oncol. Clin. N. Am. 25, 439-445.

Molina J.R., Yang P., Cassivi S.D., Schild S.E. and Adjei A.A. (2008). Non-small cell lung cancer: epidemiology, risk factors, treatment, and survivorship. Mayo Clin. Proc. 83, 584-594.

Naylor E.C., Desani J.K. and Chung P.K. (2016). Targeted therapy and immunotherapy for lung cancer. Surg. Oncol. Clin. N. Am. 25, 601-609.

Qadir M.I. and Faheem A. (2017). miRNA: A diagnostic and therapeutic tool for pancreatic cancer. Crit. Rev. Eukaryot. Gene Expr. 27, 197-204.

Smith L.L., Yeung J., Zeisig B.B., Popov N., Huijbers I., Barnes J., Wilson A.J., Taskesen E., Delwel R., Gil J., Van Lohuizen M. and So C.W. (2011). Functional crosstalk between Bmi1 and MLL/Hoxa9 axis in establishment of normal hematopoietic and leukemic stem cells. Cell Stem Cell 8, 649-662.

Song M., Sun M., Xia L., Chen W. and Yang C. (2019). miR-19b-3p promotes human pancreatic cancer Capan-2 cells proliferation by targeting phosphatase and tension homolog. Ann. Transl. Med. 7, 236.

Sun Z., Shi K., Yang S., Liu J., Zhou Q., Wang G., Song J., Li Z., Zhang Z. and Yuan W. (2018). Effect of exosomal miRNA on cancer biology and clinical applications. Mol. Cancer 17, 147.

Tang Y., Yang J., Wang Y., Tang Z., Liu S. and Tang Y. (2020). MiR-19b-3p facilitates the proliferation and epithelial-mesenchymal transition, and inhibits the apoptosis of intrahepatic cholangiocarcinoma by suppressing coiled-coil domain containing 6. Arch. Biochem. Biophys. 686, 108367.

Tutar Y. (2014). miRNA and cancer; computational and experimental approaches. Curr. Pharm. Biotechnol. 15, 429.

Wang L., Yang G., Zhao D., Wang J., Bai Y., Peng Q., Wang H., Fang R., Chen G., Wang Z., Wang K., Li G., Yang Y., Wang Z., Guo P., Peng L., Hou D. and Xu W. (2019a). CD103-positive CSC exosome promotes EMT of clear cell renal cell carcinoma: role of remote MiR-19b-3p. Mol. Cancer 18, 86.

Wei Y., Guo S., Tang J., Wen J., Wang H., Hu X. and Gu Q. (2020). MicroRNA-19b-3p suppresses gastric cancer development by negatively regulating neuropilin-1. Cancer Cell Int. 20, 193.

Xia Z., Yang C., Yang X., Wu S., Feng Z., Qu L., Chen X., Liu L. and Ma Y. (2019). miR-652 promotes proliferation and migration of uveal melanoma cells by targeting HOXA9. Med. Sci. Monit. 25, 8722-

8732.

Xu C., Li B., Zhao S., Jin B., Jiav R., Ge J. and Xu H. (2019). MicroRNA-186-5p inhibits proliferation and metastasis of esophageal cancer by mediating HOXA9. Onco. Targets Ther. 12, 8905-8914.

Yang Y., Ding L., Hu Q., Xia J., Sun J., Wang X., Xiong H., Gurbani D., Li L., Liu Y. and Liu A. (2017). MicroRNA-218 functions as a tumor suppressor in lung cancer by targeting IL-6/STAT3 and negatively correlates with poor prognosis. Mol. Cancer 16, 141.

Yuan Y., Xu X.Y., Zheng H.G. and Hua B.J. (2018). Elevated miR-21 is associated with poor prognosis in non-small cell lung cancer: a systematic review and meta-analysis. Eur. Rev. Med. Pharmacol. Sci. 22, 4166-4180.

Zhang Y., Sui J., Shen X., Li C., Yao W., Hong W., Peng H., Pu Y., Yin L. and Liang G. (2017). Differential expression profiles of microRNAs as potential biomarkers for the early diagnosis of lung cancer. Oncol. Rep. 37, 3543-3553.

Zhao L., Zhao Y., He Y. and Mao Y. (2017). miR-19b promotes breast cancer metastasis through targeting MYLIP and its related cell adhesion molecules. Oncotarget 8, 64330-64343.

Zhu Y., Li T., Chen G., Yan G., Zhang X., Wan Y., Li Q., Zhu B. and Zhuo W. (2017). Identification of a serum microRNA expression signature for detection of lung cancer, involving miR-23b, miR-221, miR-148b and miR-423-3p. Lung Cancer 114, 6-11.

Accepted March 11, 2022